Application of Nanoparticles in Synthesis of Rubber Nanocomposites

5.1 Introduction

Polymer nanocomposites are being investigated since 1980's, Gary Tibbets of General Motors Research Laboratories is widely recognized as one of the earliest investigators in the development of nanofibers and filaments for automotive applications. Toyota was the first company to synthesize clay- polymer nanocomposites and used the same as structural components in their automobiles (Usuki 1993).

Nanofillers offer equivalent or superior properties compared to traditional fillers with much lower filler loading. However, the new nanofillers are more difficult to process than conventional fillers, agglomeration of filler particles, dispersion and interaction between filler and polymer matrix are difficult to control (Kang et al. 2007, Chakravarty 2007). In recent years, tire manufacturers turned their interest towards nanofillers to meet the increased quality requirements of tires, especially of lower rolling resistance and at the same time good traction and abrasion resistance. In rubbers as in polymers the problems related to the utilization of nanofillers are similar, in addition, the mixing process of rubber is rather complicated and more difficult than polymers (Thomas et al. 2010).

The effectiveness of the filler depends on filler characteristics such as size and shape of the particles and more significantly on the strength of polymer-filler interaction. The state of dispersion is also considered to be crucial importance for the mechanical response of the materials. Carbon black is one of the most common reinforcing fillers in rubber compounding since the beginning of the 20^{th} century. Carbon black due to its unique particle dimension and shape and its special interaction with polymer matrices with physical and chemical bonding is able to produce an excellent nano-reinforcing effect that greatly enhances the mechanical properties of the bare polymer or rubber (McBrity 1991).

In last two decades much research has focused on the development of other reinforcing agents to replace carbon black in rubber compound. Clays are in use since

a very long time for the enhancement of mechanical properties of polymers and rubbers although their reinforcing effect is much less important that that exerted by carbon black. The typical approach in the utilization of clays in rubber and plastics composites was to break down clay particles aggregates into individual particles to form micro-sized fillers (Pavlidou et al.2008).

The simplest way to introduce nano- clay in a polymer matrix consists in the melt processing. The nanoclay is added in the polymer matrix during mixing stage when the matrix is in a viscous liquid –like stage. However, with this simple approach it is not possible to achieve particularly impressive reinforcing properties. Hence, in the rubber industry numerous techniques are adopted to enhance properties that include different missing techniques, use of combination fillers such as carbon black and nanoclay, surface treatment of fillers to enhance rubber filler bonding etc (Hua 2008, Bokabza 2007)).

This investigation is focused on a very specific component of a tire, its inner liner. Tires are inherently complex composite objects, cut out picture of tire shows the various structural parts of a tire. The inner liner is the innermost part of the tire that is in contact with air, this layer has to fulfill multiple objective it must provide adequate impermeability, resistance to moisture penetration, adhesion to the casing, and good crack and fatigue resistance. (Exxon Mobil 2014)

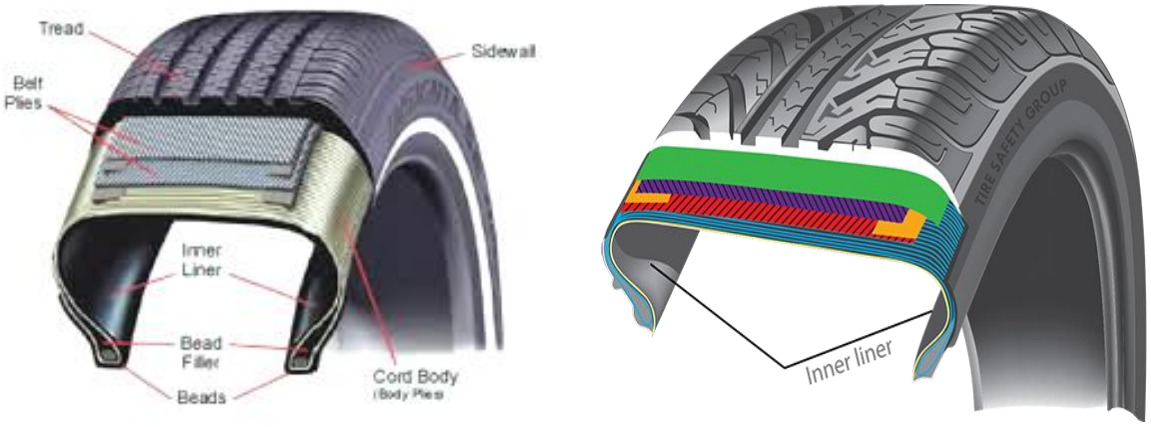

Fig. 5.1 Illustration of Inner liner in tires (Exxon Mobil 2014)

The tire inner liner can be up to 9 percent of the total tire compound weight it is therefore of considerable importance. Different types of tires have different inner liner

compounds racing car tires use natural rubber since this helps in handling requirements. Truck tires on the other hand have a mixture of natural and halobutyl rubbers, the former for stability purpose while the later to improve impermeability.

5.2 Literature Survey

A comprehensive review of literature in this vast field is difficult to achieve however, the salient aspects of halobutyl rubbers, nanoclays and its role in nanocomposite formation as well as recent trends in this area is highlighted below:

5.2.1 Halobutyl Rubbers

Isobutylene-based elastomers include butyl rubber (IIR), halogenated butyl rubber (HIIR), star-branched versions of these polymers, and brominated isobutylene-co-*para*-methylstyrene (BIMSM). Due to their impermeability and resistance to heat and oxidation, these polymers find application in tire innerliners, innertubes, curing bladders and envelopes, and other specialty applications where air retention and resistance to heat and oxidation are desired. Commercially, chlorobutyl (CIIR) and bromobutyl (BIIR) derivatives of butyl elastomers are of greater importance.

As a general guide to selecting grades of a halobutyl for varying applications:

1. Lower viscosity halobutyl is preferred for thinner liner gauges and when natural rubber will be added for green strength. An example is passenger tire innerliners.
2. Higher viscosity halobutyl is preferred when heavier liner gauges are required, i.e. when excellent air retention requirement is needed such as for commercial truck and aircraft tires. This allows better green strength to ease processing through the tire manufacturing process.
3. In blends with other general purpose elastomers, the viscosity of the halobutyl should match as close as possible the viscosity of the other elastomers for ease of processing.
4. One hundred percent halobutyl innerliners tend to use bromobutyl as it offers better cure rates for co-curing with adjacent components in the tire.

5. Chlorobutyl is preferred for blends of SBR and natural rubber. Examples would include bias truck tire liners and tube type tires where the liner can contain up to 60 phr natural rubber.

6. Star branched bromobutyl (SBB) offers improved processing and green strength properties and is interchangeable with other bromobutyl elastomers of similar viscosity.

The primary difference between bromobutyl and chlorobutyl is the greater reactivity of the C-Br bond. This results in a number of differences between these two elastomers. Bromobutyl rubber has a faster cure rate, gives a higher crosslink density per mole of halogen in the polymer, and covulcanizes better with other unsaturated rubbers.

5.2.2 Nanoclays

Clay fillers include both natural clays (Phyllosilicates e.g., montmorillonite, hectorite and saponite) and synthesized clays (e.g., fluorohectorite, laponite and magadiite). Among them, MMT and hectorite are to date the most widely used ones. Clay minerals used for polymer nanocomposites can be classified into three types; they are 2:1 type, 1:1 type and layered silicic acids. Their structures are briefly described as follows.

2:1 type: The clays belong to the smectite family with the crystal structure consisting of nanometer thick layers (platelets) of aluminum octahedron sheet sandwiched in between two silicon tetrahedron sheets. Staking of the layers lead to a van der Waals gap between the layers. Isomorphic substitution of A1 with Mg, Fe, Li in the octahedron sheets and/or Si with A1 in tetrahedron sheets gives each three-sheet layer an overall negative charge, which is counterbalanced by exchangeable metal cations residing in the interlayer space, such as Na, Ca, Mg, Fe and Li.

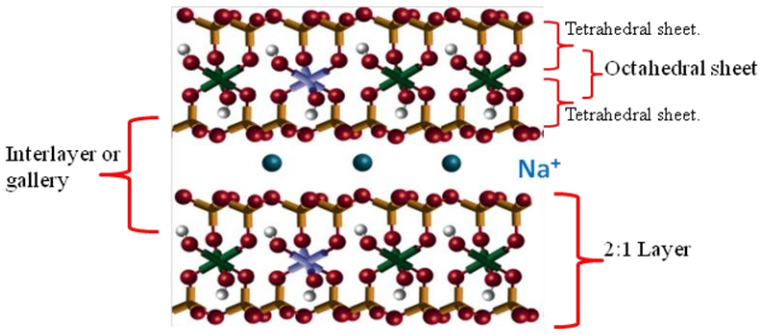

Fig. 5.2 Structure of sodium montmorillonite (Paul et al (2008))

1:1 type : The clays consist of layers made up of one aluminum octahedron sheet and one silicon tetrahedron sheet. Each layer bears no charge due to the absence of isomorphic substitution in either octahedron or tetrahedron sheet. Thus, except for water molecules neither cations nor anions occupy the space between the layers, and the layers are held together by hydrogen bonding between hydroxyl groups in the octahedral sheets and oxygen in the tetrahedral sheets of the adjacent layers.

Surface modification

The unique layered structure and high intercalation capabilities allow Clays to be chemically modified to be compatible with polymers, which makes them particularly attractive in the development of clay based polymer nanocomposites. The most popular modification for clays is to exchange the interlayer inorganic cations (e.g., Na+, Ca2+) with organic ammonium cations (Ruiz et al. 2006). Another key aspect of surface modification is to swell the interlayer space up to a certain extent (normally over 20 A) and hence reduce the layer-layer attraction, which allow a favorable diffusion and accommodation of polymer or precursor into the interlayer space.

5.2.3 Types of nanocomposites

When layered clays are filled into a polymer matrix, either conventional composite or nanocomposite can be formed depending on the nature of the components and processing conditions. Conventional composite is obtained if the polymer cannot intercalate into the galleries of clay minerals. The properties of such composite are similar to that of polymer composites reinforced by micro particles. Depending on the strength of interfacial interaction between elastomer matrix and nanofillers (modified or not), three different types of nanocomposites are thermodynamically achievable.

a. Intercalated nanocomposites: In intercalated nanocomposites, the insertion of rubber matrix into the layered nanofiller occurs in a crystallography regular fashion, regardless of the clay to rubber ratio. Intercalated nanocomposites typically resemble those of ceramic materials.

b. Flocculated nanocomposites: conceptually this is same as intercalated nanocomposites. However, filler layers are some time flocculated due to hydroxylated edge-edge interaction of the fillers layers.

c. Exfoliated nanocomposites: In an exfoliated nanocomposite, the individual clay layers are separated in a continuous rubber matrix by an average distances that depends on clay loading, the clay platelets are completely and uniformly dispersed in a continuous polymer matrix.. Usually, the clay content of an exfoliated nanocomposite is much lower than that of an intercalated nanocomposite. However, it should be noted that in most cases the cluster (so-called partially exfoliated) nanocomposite (III) is common in polymer nanocomposites. Fig 5.3 exhibits the morphology observed in all these states.

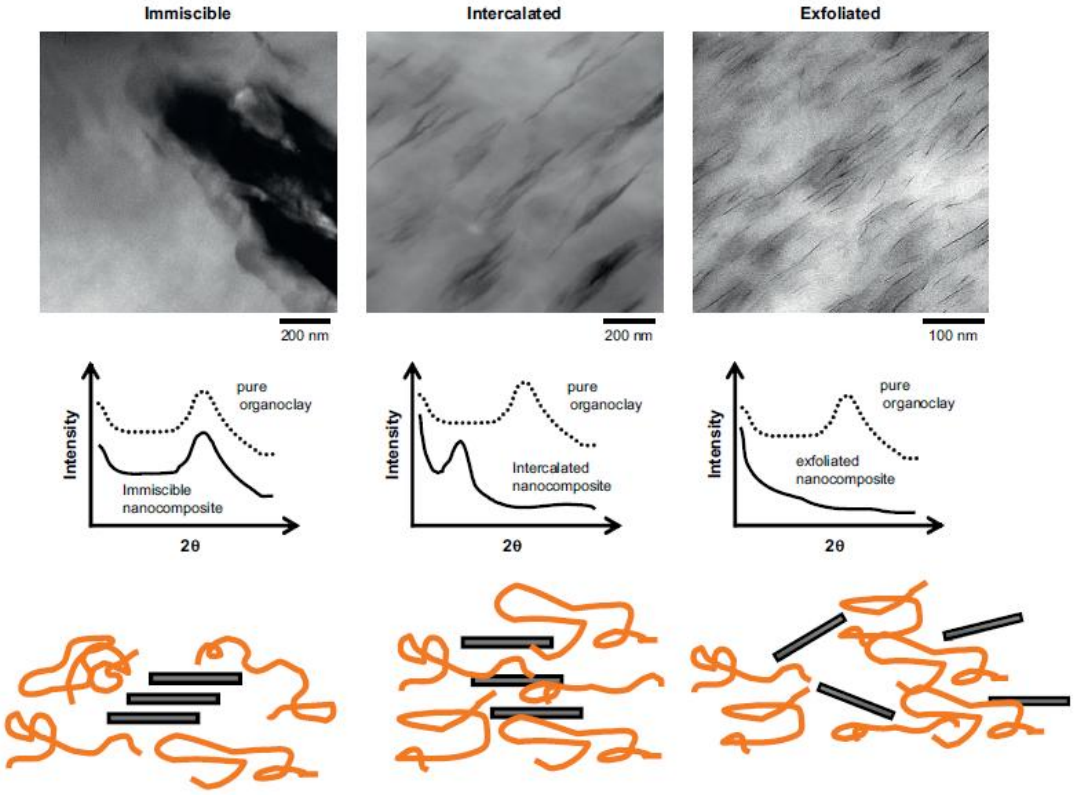

Fig. 5.3 Illustration of different states of dispersion of organoclays in polymers with corresponding WAXS and TEM results(Paul et al (2008))

5.2.4 Salient Investigations

Sinha Ray and Okamodo (2003) have reviewed polymer/layered silicate nanocomposites from preparation to processing. The academic and industrial aspects

of the preparation, characterization, materials properties and crystallization behavior, melts rheology and processing of polymer/layered silicate nanocomposites is discussed.

Sadhu and Bhowmick (2004, 2005) have studied on factors influencing the morphology and the properties of clay-rubber nanocomposites. The effects of the type of clay, the modifier used and the loading as well as the nature of the rubber, the processing and curing conditions, on the morphology, mechanical and dynamic mechanical properties of various rubber nanocomposites was discussed. Most of the rubber-clay nanocomposites display best physic-mechanical properties at a nanoclay loading of 4 phr. The improvement in properties is due to exfoliation of the fillers. Interestingly, a few rubbers also could exfoliate unmodified clay, thus leading to enhanced properties of the nanocomposites. The extent of increase of tensile strength and modulus is often 200% depending on the polarity of rubber, clay structure etc. Distinctly different morphologies have been obtained when melt and solution intercalation techniques are compared, particularly evident for thermoplastic elastomers based on block copolymers.

Pal et al. (2009) studied the blends of higher styrene rubber (HSR) and natural rubber with nano silica were The blends of high styrene rubber (HSR) and natural rubber (NR) with nano silica were prepared using a blending technique in presence of different types of carbon black. The effect of filler on morphological and wear characteristics was studied. ISAF (Intermediate Super Abrasion Furnace) type of carbon black have showed a significant effect on optimum cure time, cure rate index and mechanical properties by reacting at the interface between HSR and NR matrix. All the samples show only melting peak on the DSC curve; this is attributed to the same backbone structure of the matrix and the carbon black reinforcement. The samples containing 30 wt% of HSR with ISAF type of carbon black has shown maximum heat buildup, lower swelling and lower compression set value. Blends containing ISAF type of carbon black with 30 wt% of HSR showed high abrasion resistance properties against Du-Pont abrader, DIN abrader and different mining surfaces and also found to be toughest rubber against all types of rocks.

Pal et al. (2009, 2010), have reported an Influence of fillers on NR/SBR/XNBR blends. The blends of carboxylated acrylonitrile butadiene rubber

(XNBR), styrene-butadiene rubber with high styrene content (SBR) and natural rubber (NR) were prepared with different types of carbon black. The effect of filler on morphological and wear characteristics was studied. Intermediate super abrasion furnace (ISAF) carbon black showed improve result on curing study and mechanical properties by reacting at the interface between XNBR, SBR and NR matrix. Blends containing ISAF carbon black showed higher abrasion resistant properties against Du-Pont abrader, DIN abrader and different minimum surfaces and also is found to be toughest rubber against all types of rock.

Susteric et al. (2010) have studied dynamic mechanical properties of non-polar and polar elastomer-based nanocomposites with montmorillonite clay are studied in order to ascertain differences caused by elastomers polarity. Natural as non-polar and polychloroprene as polar rubber are used to experimentally verify predictions based on different nature of elastomer-clay interactions in the two cases. The properties foretold and elucidated in terms of van der Waals interactions in the non-polar case and dipole-dipole interactions in the polar case agree well with experiment, concurrently sustaining general depiction of these unusual nanocomposites.

In a series of investigation Ghosh et al. tried to address issues related to rolling resistance in tyres, that is responsible for considerable loss of energy and leads to enhanced fuel consumption and environmental stress. Ghosh et al. (2011) investigated the high performance nanocomposites prepared from blends of SBR and BR they prepared n anocomposites based on SBR/BR blends and organoclay (Cloisite15A) in presence of carboxylated nitrile rubber (XNBR) used as compatibiliser by employing a solution process as well as mechanical mixing on two-roll mill and internal mixer. The dosage of organoclay and XNBR was optimized and the nature of SBR varied. The mechanical properties of nanocomposites improve as the carboxyl group content in XNBR increases. Highly exfoliated structure of clay and excellent mechanical properties were obtained by all three mixing techniques, however internal mixer showed the best properties and 2 rolls mill mixing was the most difficult.

Later Ghosh et al. (2011) evaluated tire rolling resistance of 205/60R15 passenger car radial tire with nanocomposite based tread compounds using finite element (FE) analysis. The energy dissipation in the tire was evaluated using the

product of elastic strain energy and the loss tangent of materials through post processing using a rolling resistance code. Nanocomposites used in this study were prepared based on solution styrene butadiene rubber (SSBR) and polybutadiene rubber (BR) blends with either organoclay and carbon black or organoclay and silica dual fillers. Carboxylated nitrile rubber (XNBR), a polar rubber, was used as compatibilizer to facilitate the clay dispersion in rubber matrix. Compared to general carbon black or silica tread compounds, substantial improvement of rolling resistance was predicted by FE simulation with nanocomposite based tread compounds containing dual fillers organoclay-carbon black or organoclay – silica.

Finally Ghosh et al. in 2014 reported nanocomposites based on Natural Rubber (NR) and Polybutadiene Rubber (BR) blends with either organoclay and carbon black or organoclay and silica dual fillers system and used it in conjunction with a rolling resistance code to predict rolling resistance of Truck Bus Radial (TBR) tyres with nanocomposite based tread compounds. The energy dissipation in the tyre was evaluated approximately using the product of elastic strain energy and loss tangent of materials through post-processing using a rolling resistance code. The elastic strain energy is obtained through steady state rolling simulation of tyres using commercial software. The loss tangent vs. strains at two reference temperatures is measured in the laboratory using a dynamic mechanical thermal analyzer. A temperature equation is developed to incorporate the effect of temperature on loss energy i.e. rolling resistance. A good correlation of rolling resistance is observed between simulation and experimental results. Compared to general carbon black or silica tread compounds, substantial improvement of rolling resistance is predicted by FE-simulation with nanocomposite based tread compounds containing dual fillers.

5.3 Materials and Methods

5.3.1 Materials and Ingredients

Natural rubber and Bromobutyl rubber used in these studies were supplied by Appolo tires which were imported from Polymer Latex (Selangor, Malaysia). Other ingredients [sulfur, zinc oxide, MBTS Accelerator, 6 PPD and antioxidant] were supplied by Farben Technique (M) (Sendirian Berhad, Penang, Malaysia). The fillers

used in this study Carbon Black was supplied by Birla Chemicals, India and Nanoclay from Nikko Kogyo Co. (Tokyo, Japan) .

The particle size distribution of nanoclay measured using Malvern 2000 mastersizer Laser particle size analyzer is given below in Fig. 5.4 the clay showed unimodal distribution having average particle size of 10 μm which were obviously aggregates. Carbon black showed bimodal distribution with two range of particle sizes the lower one having mean of 10 μm and larger one having a mean at 200 μm.

All materials were used as supplied.

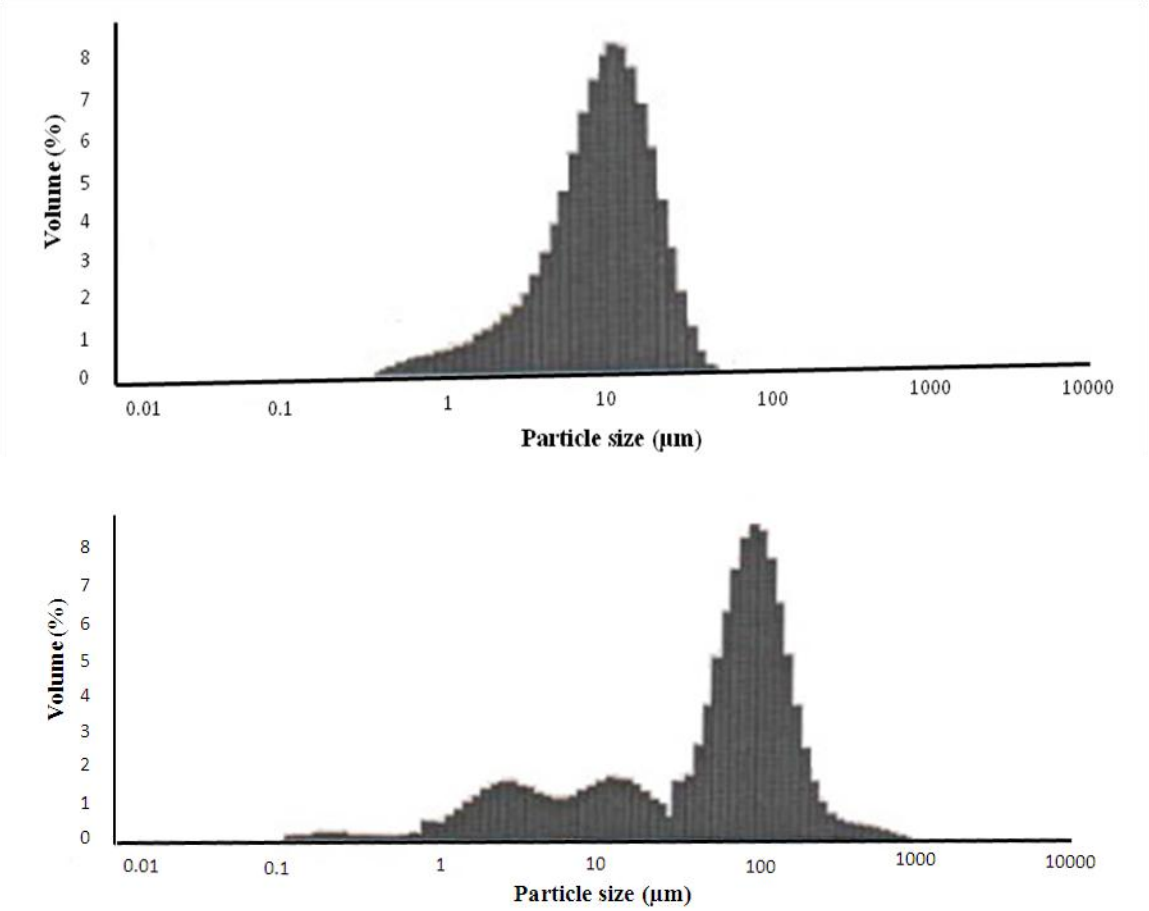

Fig. 5.4 Particle size distribution of Fillers.

5.3.2 Compounding

Compounding of the rubber was done in laboratory mixer. Rubber mixing was carried out in accordance with ASTM D3184 using a laboratory sized banbury mixer. The various rubber additives were added to the masticated natural rubber prior to the addition of organoclay and other ingredients.

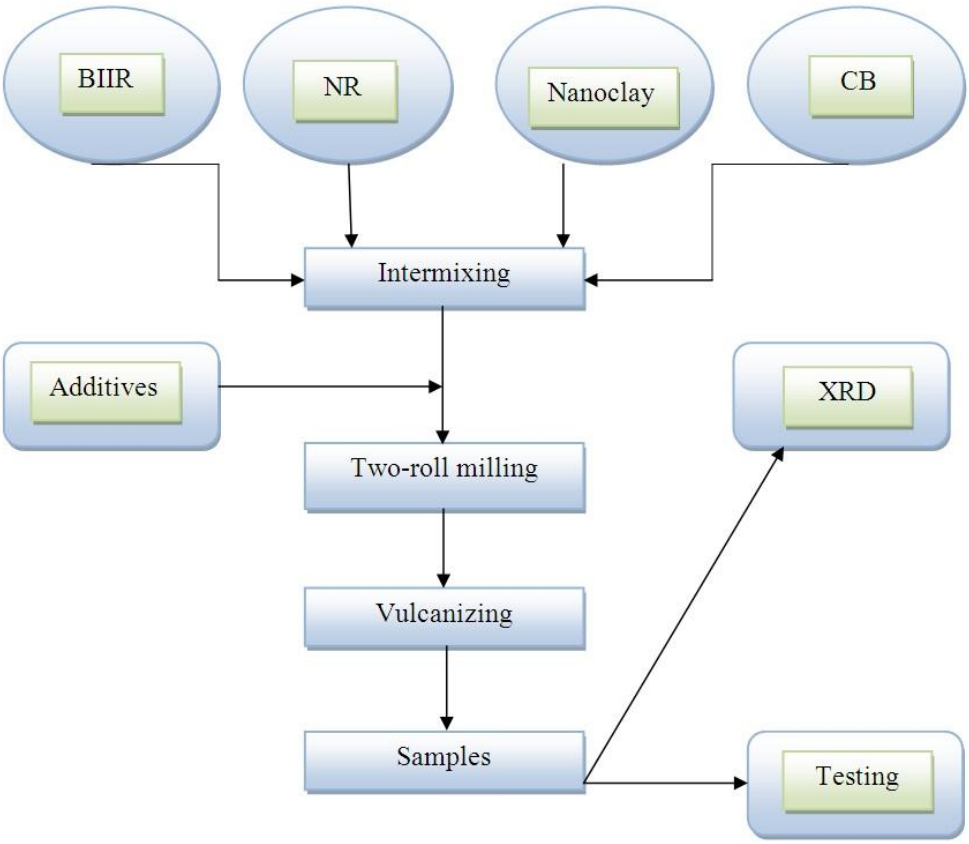

Fig. 5.5 : Experimental flow chart.

After sheeting the rubber foils were rolled and passed in the mill put the roll in the same direction of motion of the rotors in order to impart a preferential direction to the filler. All specimens were prepared and tested according to the standard ASTM. The following is a flow chart of experiments.

The compounding ingredients and amount used for this study are presented in Table 5.1.

Table 5.1 : Formulation for the NR/BIIR compounding

Compound	M0	M1	M2	M3	M4	M5
Bromo butyl rubber (BIIR)	60.00	60.00	60.00	60.00	60.00	60.00
Natural rubber (RSS-III)	40.00	40.00	40.00	40.00	40.00	40.00
Zinc oxide	3.0	3.00	3.00	3.00	3.00	3.00
MBTS Accelerator	1.50	1.50	1.50	1.50	1.50	1.50
6PPD	1.00	1.00	1.00	1.00	1.00	1.00
Stearic acid	1.00	1.00	1.00	1.00	1.00	1.00
Soluble sulphur	0.50	0.50	0.50	0.50	0.50	0.50
Carbon black (GPF)	-	40.00	30.00	20.00	10.00	0.00
Clay	-	0.00	2.00	4.00	6.00	8.00
Peptizer	0.10	0.10	0.10	0.10	0.10	0.10

The nanoclay was used in the above formulation at 2, 4, 6 and 8 phr respectively. Naturally, a "blank" reference compound without nanoclay was mixed as well.

5.3.3 Test Methods

Hardness

Testing was done with Durometer Hardness Tester according to ASTM-D2240, Shore A method. The thickness of the material was ensured up to 4 mm. The hardness after 15 seconds was recorded. The test was done under normal laboratory conditions.

Tensile Test

Tensile test was done according to ISO. The tensile test was carried out with Zwick Universal testing Machine at a cross head speed of 50 mm/min. The testing machine used is equipped with suitable grips suitable for rubber testing. The test was done under normal laboratory condition.

Tear strength

The tear strength was tested with same equipment as the tensile properties: The Zwick Universal Tensile testing machine. The test was done according to ISO. The tear strength was measured in the milling direction. Testing was conducted under normal laboratory conditions.

Rheological Measurement

The cure characteristics of the rubber compound were studied with help of a MDR 2000E, Alpha Technology, USA at 160C per ASTM-D-2084-07. From the graphs the optimum cure time scorch time and rate of cure (tmax, tmin) were determined.

Dynamic Mechanical Analysis

Dynamic Analysis (DMA) measures the response of a material to cyclic deformation (usually tension) as function of the temperature. DMA results are expressed by three main parameters:

1. The storage modulus (E') corresponding to the elastic response to the deformation;
2. The loss modulus (E") corresponding to plastic response to the deformation;
3. Tan δ, that is E'/E" ratio, useful for determining the occurrence of molecular mobility transitions such as the glass transition temperature.

X-ray diffraction (XRD)

X-ray diffraction (XRD) was used for characterization of the rubber nanocomposites using Rigaku CN2005 X-Ray Diffractometer, Miniflex model in the range of 10^o to 50^o (=2Θ).

The basal spacing of the nanoclay and nanocomposite was evaluates using wide angle X-ray diffraction in a Phillips X-pert Pro diffractometer (PANalytical, Eindhoven, NL) at narrow angular range of 2^o to 10^o using Cu-Kα radiation (K= 0.154 nm). In these studies the acceleration voltages of 40 kV and beam current of 30 mA was used. The scanning rate was maintained at 1.5^o per minute. The d-spacing of the particles were calculated using the Bragg's law.

Transmission Electron Microscopy (TEM)

The microstructure of the nanocomposite was imaged using transmission electron microscopy. Ultrathin sections of 300 nm thickness of the nanocomposites were cut by ultra microtome at ~ -80^o C (below the glass transition temperature T_g of rubber) and the images were taken by JEOL JEM 2100 (Japan) with an acceleration voltage of 200 kV and resolution 1.4A.

Atomic Force Microscopy (AFM)

The microstructure of the nanocomposite was studied under scanning probe microscope for high resolution measurement of atomic image. The instrument employed was AGILENT TECHNOLOGIES 5500 with cantilever resonant frequency 160KHz, force constant 21(N/m), tip material SiN, TIP radius of curvature <10 nm and cantilever length <100 micron. The software used is PICO IMAGE BASIC.

5.4 Results And Discussions

The objective of this work was to study the behavior of nanocomposites of halogenated rubber particularly Bromobutyl rubber / Natural rubber (BIIR/NR) composite. In view of this different samples were prepared with the formulation given in the Table-5.1. In all the samples the rubber matrix composed of 60 phr BIIR and 40 phr NR. It is well known that addition of natural rubber has a detrimental effect on impermeability but it helps improve green strength, resistance to cord pull-through and help address handling requirements. This matrix formulation would be appropriate for passenger car as well as truck bus tire inner liners.

5.4.1 Mechanical Properties

The effect of fillers on mechanical properties that characterize the nanocomposites are detailed and discussed below:

Hardness, Tensile strength and elongation

Hardness of rubber nanocomposites was maximum with carbon black loading of 40% and declined when the carbon black content was decreased as shown in Figure 5.6. Interestingly a linear relationship appears between amount of filler and the hardness. 40 phr carbon black contributed to 18 MPa increase in hardness and 8 phr nanoclay contributes to 12 MPa increase in hardness therefore it is expected that 20 phr of carbon black + 4 phr nanoclay would contribute half this amount i.e. 9 MPa for carbon black and 6 MPa for nanoclay totaling to 15 MPa increment in hardness and that is seen for sample M3, which has hardness of 57 Mpa compared to 42 MPa hardness of gum sample. Nanoclay reinforcement is reasonably good even at low filler loading, the problem however is to incorporate nano filler in the rubber matrix.

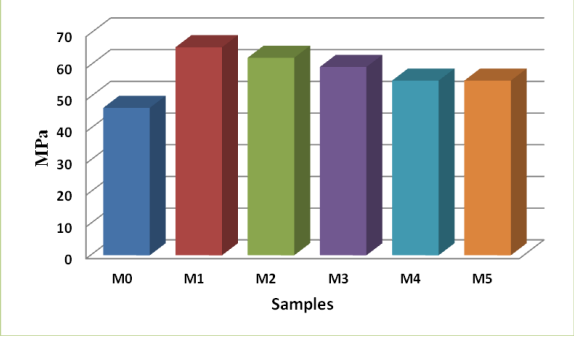

Fig. 5.6 Hardness v/s Filler loading

As already anticipated the addition of the nanoclay to the standard rubber compound boosts up the tensile strength of the compound. This is illustrated in Figure 5.7 where the tensile index values are reported. The tensile strength increases considerably in the presence of nanoclay than in the presence of carbon black and over here also we find a more or less linear relationship existing between tensile strength and mixed filler loading. Same is the case with tear strength, but we observe that carbon black influences tear strength more significantly than nanoclay.

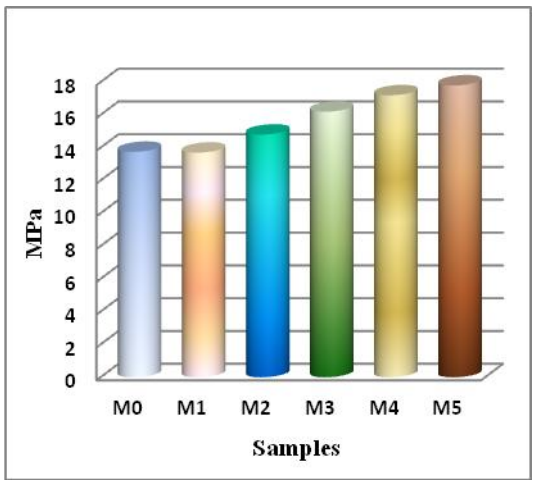

Fig. 5.7 Tensile strength v/s Filler loading

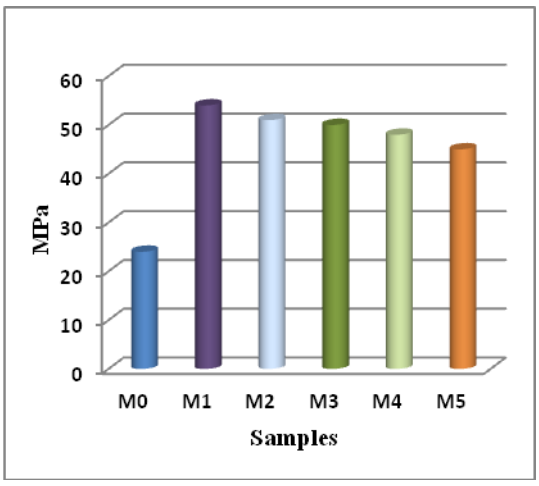

Fig. 5.8 Tear strength v/s Filler loading

The addition of the nanoclay causes a gradual increase in the elongation at break (E_B) which grows as function of the amount of the nanoclay added. As carbon black amount in the nanocomposite declines the samples become progressively more elastic and the E_B almost reach up to that of gum rubber in Sample M5 in the absence of carbon black.

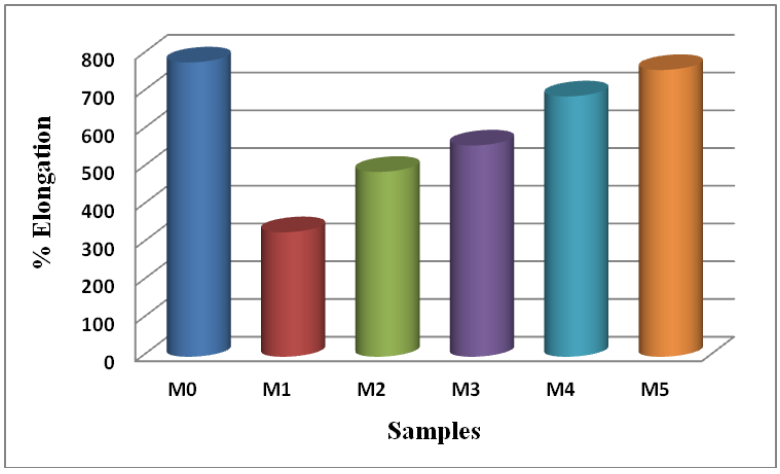

Fig. 5.9 Elongation break v/s Filler Loading

The tensile modulus at 100% (M_{100}) to 300% (M_{300}) deformation for the various samples is listed below:

Table 5.2. : Modulus and Tear strength of samples

Sample	M_0	M_1	M_2	M_3	M_4	M_5
M_{100} (MPa)	0.47	2.73	1.64	1.43	1.36	1.22
M_{200} (MPa)	0.76	7.30	3.80	3.39	2.43	1.95
M_{300} (MPa)	1.20	12.06	7.02	6.09	3.93	2.70
Tear Strength (N/mm)	21.97	49.4	48.39	48.38	47.77	40.03
Tear Work (J/mm^2)	0.723	0.99	1.15	1.35	1.93	1.44

The data presented in Table 5.2 reveals the rigidity that arises in the rubber compound in presence of large amount of filler as carbon black content declines the rubber regains its elastomeric nature. The tear strength in presence of carbon black is almost constant but declines considerably in its absence, when only nanoclay is present in sample M_5, this justifies the use of dual fillers in inner liner of tires. The tear work passes through maxima again suggesting the advantage of using a dual filler in inner liner compound.

5.4.2 Rheological Properties

Rheological data is important for rubber nanocomposites. Rheological data gives an idea of minimum and maximum torque by which various processing parameters viz. moulding pressure, extruder rpm, processing temperature etc are decided. The rheometric data also indicates the cure kinetics and the optimal cure time. The data was obtained using a moving die rheometer (MDR 2000E, Alpha Technology, USA) at 160^oC for a period of 30 minutes. A typical profile with relevant parameters of the curve is shown below in all filler loaded samples M_1 to M_5 plateau was reached in 6 minutes time for gum samples it took ~ 10 minutes.

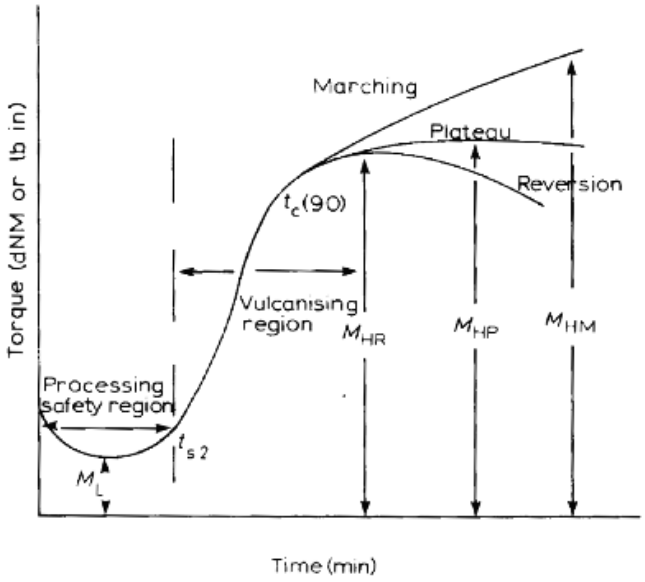

M_L = minimum torque
M_{HM} = maximum torque at specified time of marching modulus curve
M_{HP} = maximum torque at plateau curve
M_{HR} = maximum torque at reversion curve
t_{s2} = time for 2 lbf in rise above M_L used with 3° arc
$t_{c(90)}$ = time to 90 % of maximum torque

Fig. 5.10 Typical profile of cure curve

The crosslinking and cure characteristics of the various nanocomposite samples are shown in Fig 5.11 to 5.13. As filler loading declines there is a decline in both minimum torque M_L as well as maximum torque M_H. There is an increase in the processing safety region as indicated by the scorch time (Ts2) in presence of nanoclay

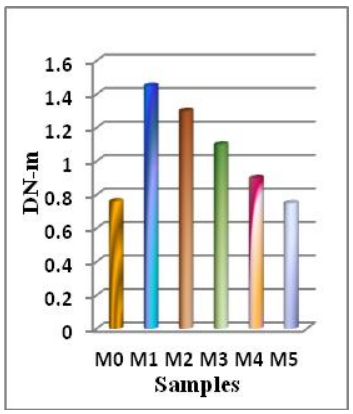

Fig. 5.11
ML v/s Filler Loading

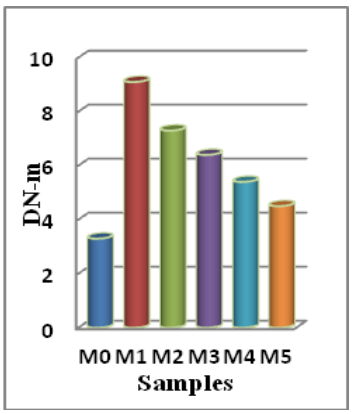

Fig. 5.12
MH v/s Filler Loading

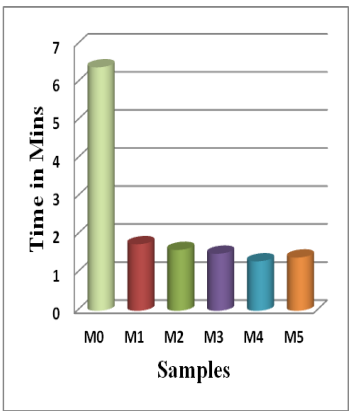

Fig. 5.13
TS_2 v/s Filler Loading

As expected, the addition of nanoclay to the rubber compound causes faster curing as indicated by the torque development time Tc10, Tc50, Tc 90. It is evident from Fig 5.14 that curing is faster in presence of nanoclay in comparison with carbon black.

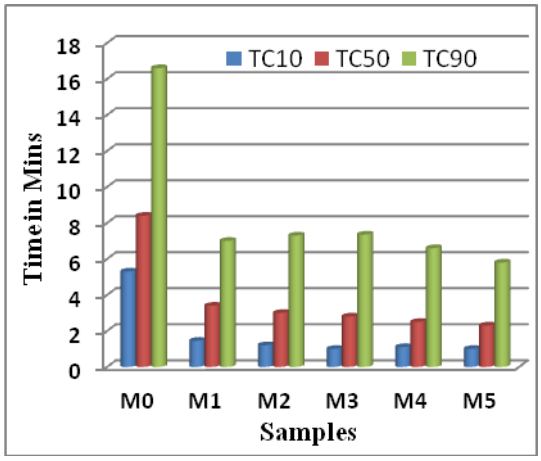

Fig 5.14 (Tc10,Tc50,Tc 90)

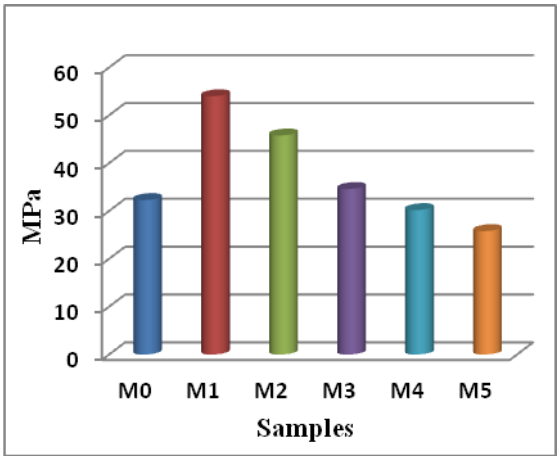

Fig. 5.15 MV v/s Filler Loading

Similarly Mooney viscosity (MV) also shows decrease in value with the substitution of carbon black with nanoclay indicating a rubber which has ease in its processability, this behavior is attributed to the greater homogeneity of the rubber matrix as carbon black component declines and nanofiller loading increases.

5.4.3 Viscoelastic Properties

The initial study of viscoelasticity concerned itself with the response of a polymer to a non-cyclic deformation imposed at either a constant strain or a constant strain rate. It was found that the elastic response is proportional to the strain level and the viscous response is proportional to the strain rate. Rubber products, however, function under conditions of cyclically varying stress or strain rates and amplitudes. To correlate the viscoelastic properties of a rubber to its performance in a product, these properties must be measured under dynamic conditions. These dynamic properties are frequently determined by measuring the response of a rubber compound to a sinusoidally varying strain. In this manner, both the strain amplitude and the strain rate vary during a complete cycle. Under these vibratory conditions, a rubber absorbs energy which is partially stored, as in a spring; and partially dissiptated in overcoming internal friction, as in a dashpot. The ratio of the energy dissipated to the energy stored is a function of the viscoelastic properties of the rubber, the temperature

of the rubber, the degree of deformation and the rate of deformation. Although most rubber products do not experience a true sinusoidal deformation, it is still possible under conditions of low deformation, to relate the response of a rubber to a sinusoidal vs. a non-sinusoidal deformation.

Viscoelastic properties of nanocomposites were determined by dynamic mechanical measurement at two temperatures 30^{o}C and 60^{o}C. The dynamical properties such as storage modulus (G$^{'}$), loss modulus (G"), Tan δ and loss compliance (J) have great influence on the performance of the nanocomposites during application. Tan δ which is the ratio of loss modulus to storage modulus of the compound i.e the ratio of viscous response to elastic response of the material represents the hysteresis loss of the compound. Hysteresis loss is greatly influenced by filler-filler interaction, higher the filler-filler interaction higher will be the hysteresis loss.

At low strains strong filler aggregates gives very high modulus that starts decreasing as the filler aggregates break down as the strain levels increases. This behavior is known as Payne's effect and is a measure of filler-filler interaction. Ghosh (2011) investigated the filler–filler interaction and observed that dual filler nanocomposites have much lower Payne's effect compared to single filler systems, primarily due to lesser amount of filler added to the compound in the former case.

The variation of the viscoelastic properties at two temperatures is of utmost importance because 30^{o}C may be considered as ambient temperature while 60^{o}C ma be the temperature attained in the inner liner of a tire due to viscous heat dissipation during rolling. Moreover, Tan δ at 60^{o}C is a measure of the rolling resistance of the tire. The loss modulus as well as the storage modulus both decline significantly with temperature, but the decline is sharper in the loss modulus. At 30^{o}C the Tanδ values are sensitive to filler loading and decreases as the loading decreases, but it becomes insensitive to filler loading at 60^{o}C which is attributed to the softening of the polmer matrix at higher temperatures. The loss compliance of the nanocomposites are not very sensitive to temperature and shows an increasing trend with the decrease in filler loading.

As seen in Figure 5.16 and 5.17 with increase in filler loading and increase in temperature storage moduli and loss moduli shows decreasing pattern.

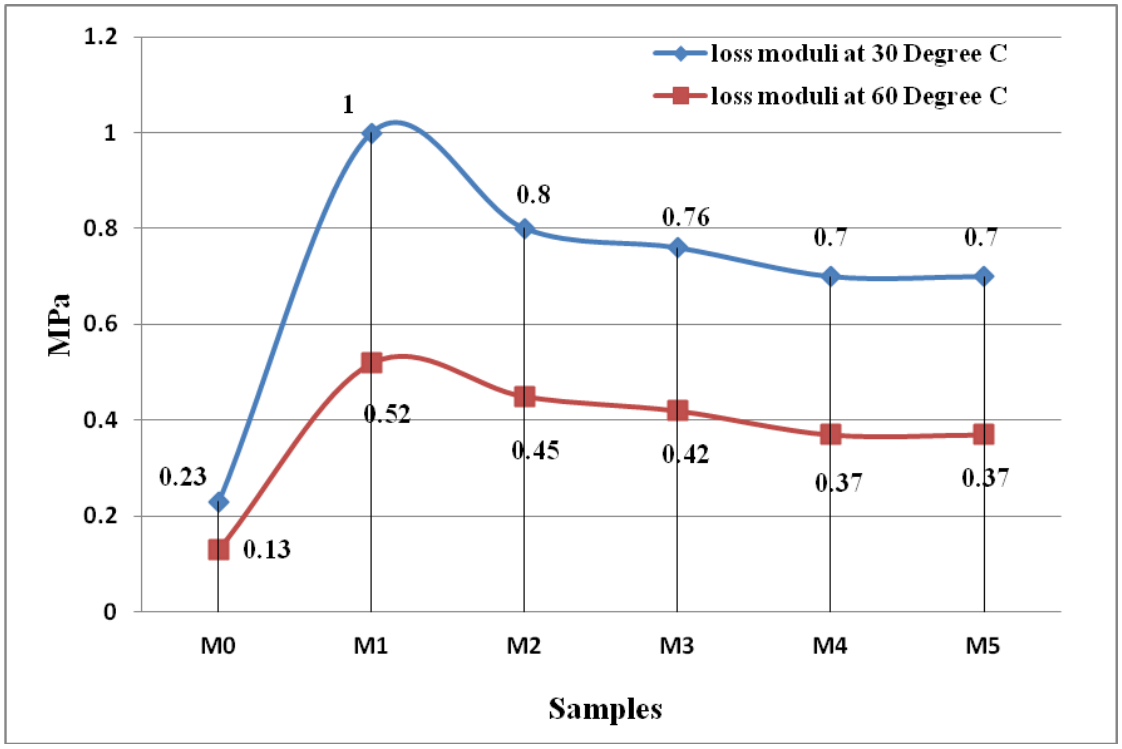

Fig. 5.16 Loss modulus v/s Filler Loading

(series 1 : loss moduli at 30°C; series 2 : loss moduli at 60°C)

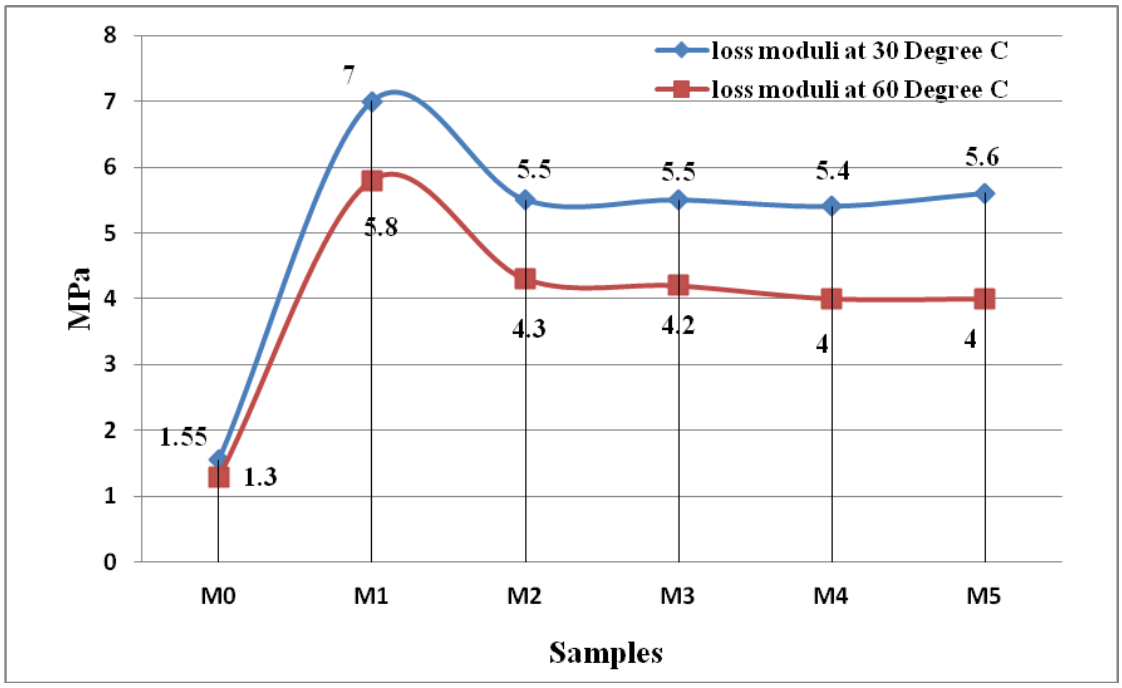

Fig. 5.17 Storage modulus v/s Filler Loading

(Series1: storage moduli at 30°C; series 2: storage moduli at 60°C)

Knowledge of the ratio Tan δ of a rubber vulcanizates is useful for understanding the distribution of elastic and viscous components. Knowledge of Tan δ will also be useful in determining how much heat will be produced in dynamic applications; too much heat could destroy a product. An example of the use Tan δ would be its value in a tire compound. A high Tan δ gives a tire tread with better traction against a road surface and therefore improved braking in the wet. This will usually be at the expense of fuel consumption, since there is more rolling resistance to movement of the automobile.

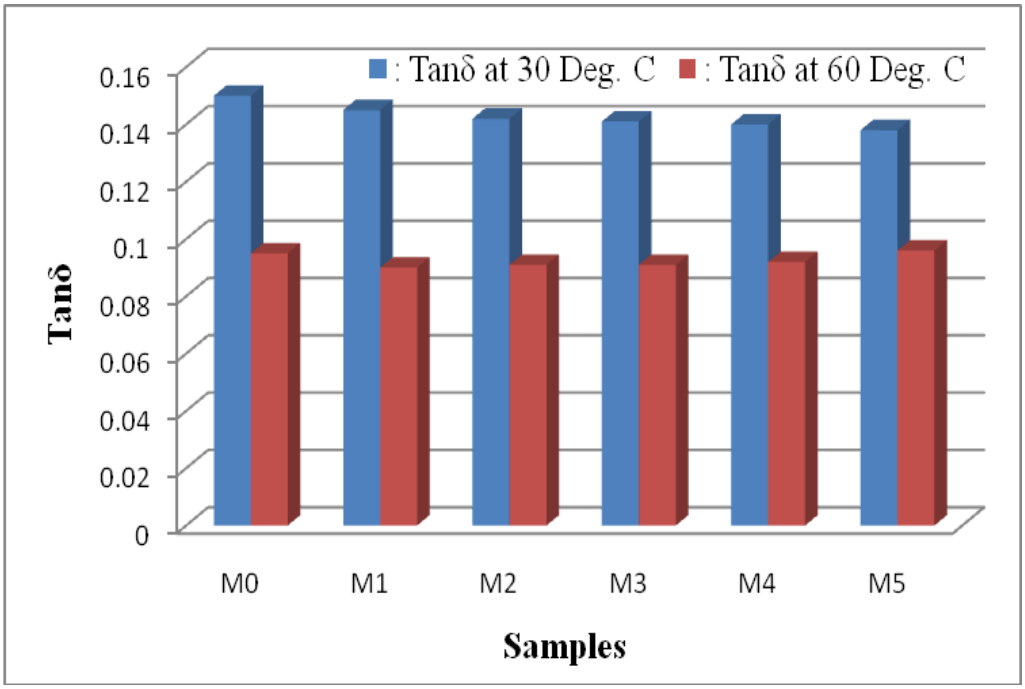

Fig. 5.18 Tan δ v/s Filler loading
(series 1 : Tan δ at 30^{o}C; series 2; Tan δ at 60^{o} C)

The value of Tan δ also shows decreasing trend with increase in filler loading. This is illustrated in Figure 5.18. The loss compliance (J) is the ratio of viscous strain amplitude to the stress amplitude shows decrease in value with increase in temperature and also with increase in filler loading. This is illustrated in Figure 5.19. This indicates that with added filler the rubber tends to become less flexible.

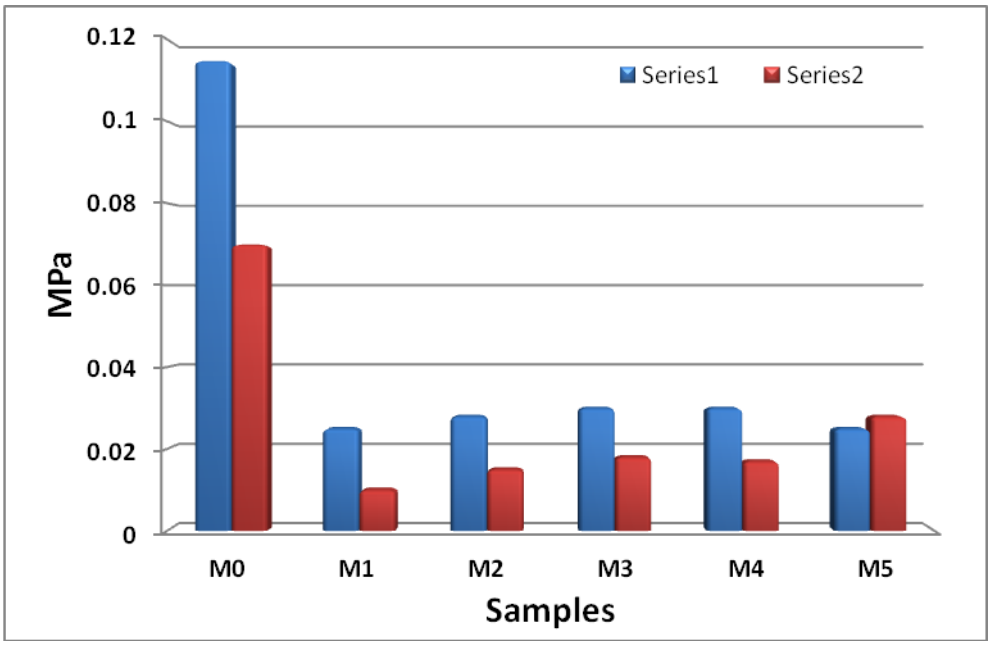

Fig. 5.19 Loss compliance v/s Filler loading

(series 1 : Loss compliance at 30^{o}C and for series 2 at 60^{o} C)

5.4.4 XRD Patterns

X-ray diffraction patterns of the gum rubber and nanocomposites is shown in Figure 5.20. In the 2ɵ range of 10^{o} to 50^{o} the diffraction patterns of gum rubber and the nanocomposites is largely the same and specific influence of the presence of the fillers cannot be distinctly discerned. Wide angle X-ray diffraction (WAXD) was performed on the nanocomposite M5 containing 8 phr of nanoclay and the same is compared with the diffraction pattern of the nanoclay as shown in Fig 5.21. This study was conducted to get an idea of the intercalation of clay in the rubber matrix b measuring gallery gap between clay layers in the nanocomposite sample. It is seen from the Fig. 5.21 that the sample has three characteristic peaks at around 2.27^{0}, 4.6^{0} and 6.42^{0} having basal spacing of 3.893 nm, 1.917 nm and 1.379 nm respectively. The basal spacing value of nanoclay obtained experimentally and from the literature of the supplier is 3.15 nm. The increase in the basal spacing d_{001} of the nanocomposite sample shows that the clay has intercalated in the rubber matrix.

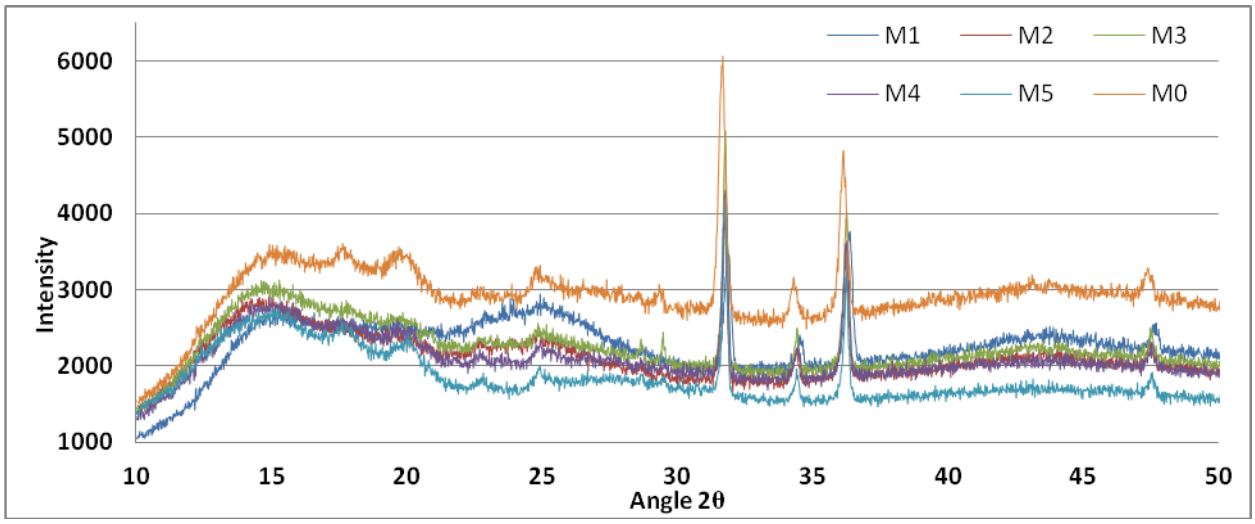

Fig. 5.20 XRD of all samples

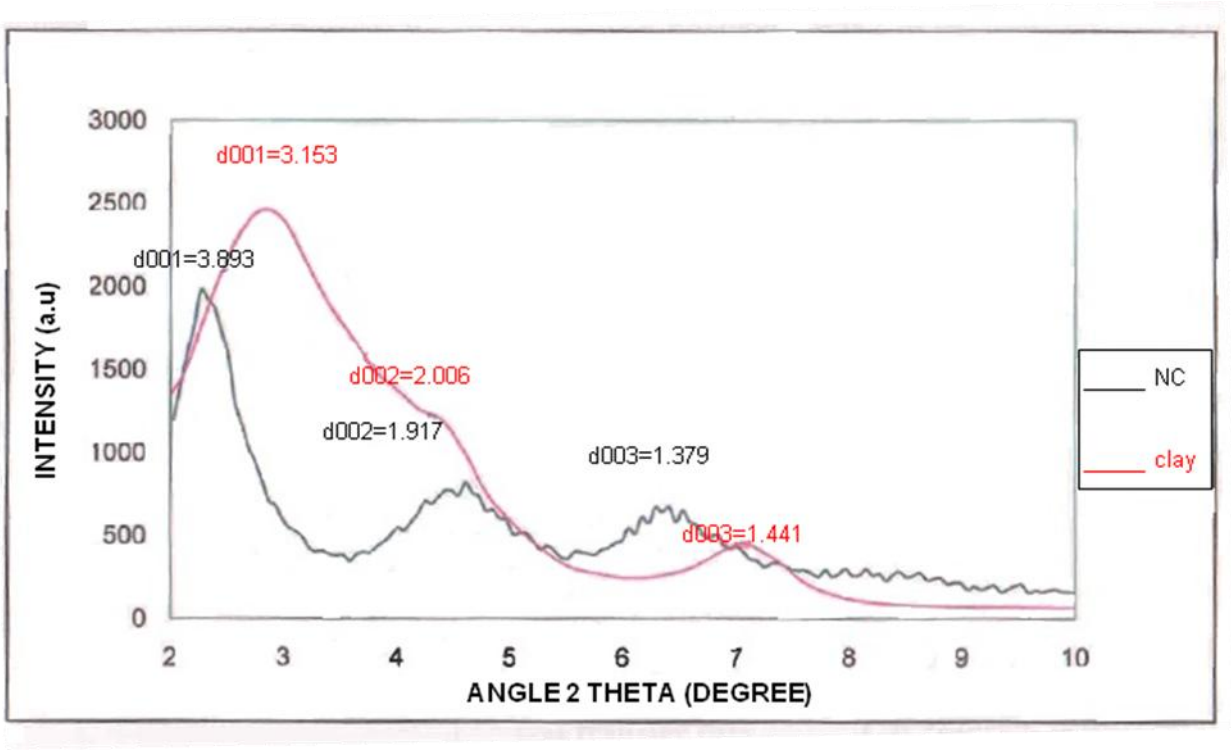

Fig. 5.21 WAXD of Nanocomposite sample M5

5.4.5 Transmission electron microscopy

The filler dispersion in the nanocomposites was studied by transmission electron microscopy (TEM). TEM images of ultrathin sections of nanocomposites of NR/BIIR are shown in Fig 5.22 to Fig 5.26 for samples M1 to M5 respectively at magnifications of 200 nm.

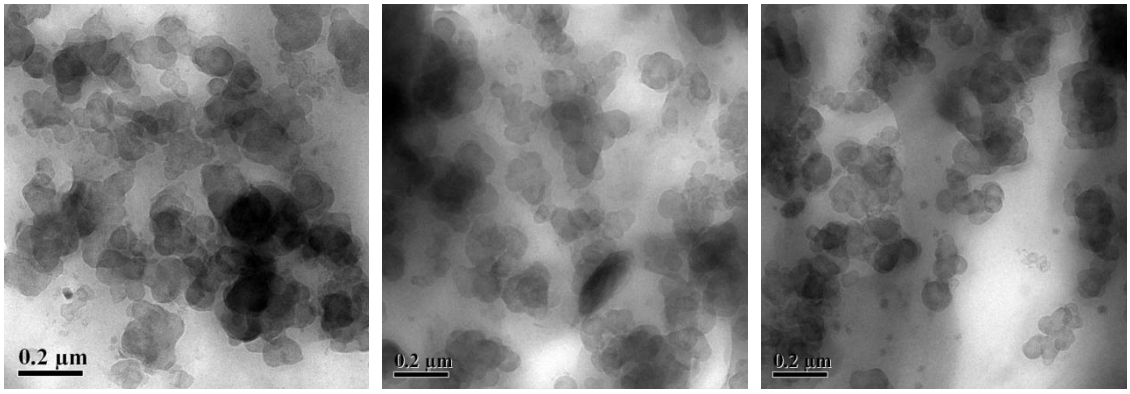

Fig. 5.22 TFM pictures of Sample M1

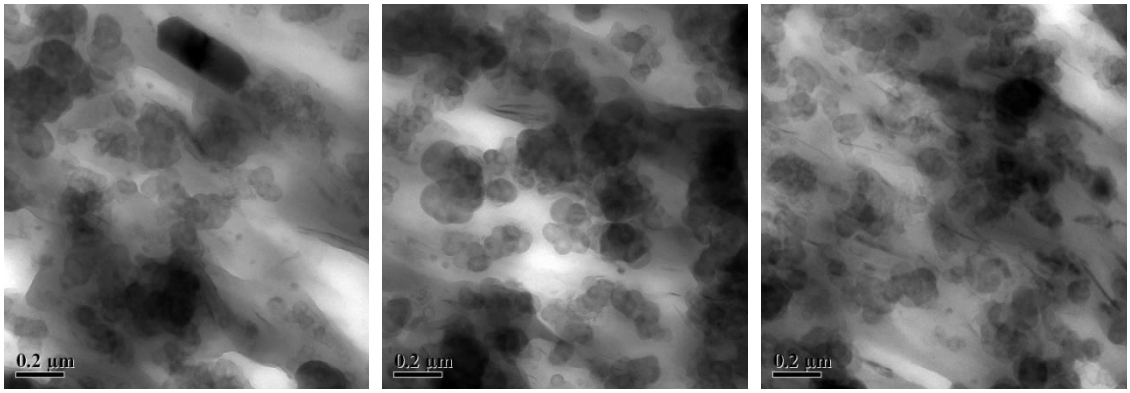

Fig. 5.23 TFM pictures of Sample M2

The light region in these images is the soft rubber matrix while the dark region is the filler since sample M1 and M2 are largely loaded with carbon black 40% and 30% respectively therefore we find agglomerates of fillers in the rubber matrix.

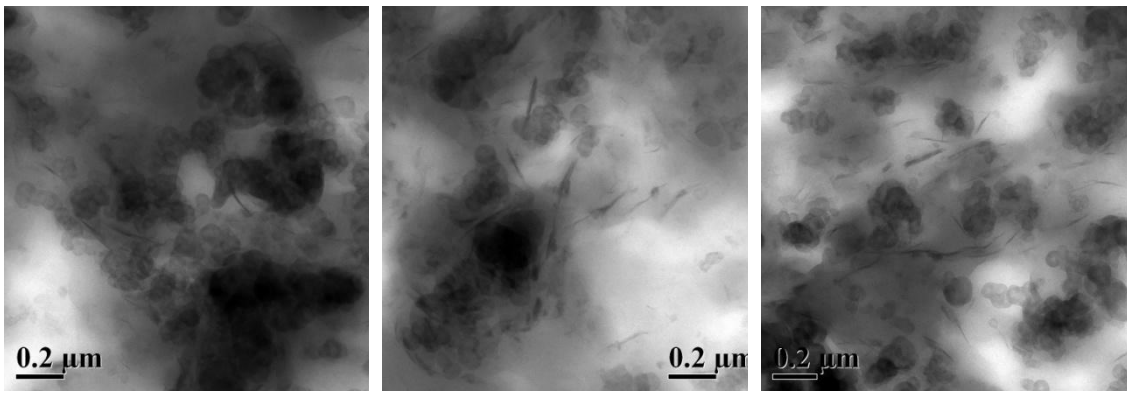

Fig. 5.24 TFM pictures of Sample M3

Sample M3 contains 20% carbon black and 4% nanoclay hence, we find that in the rubber matrix the overall filler density is less and some dark filamentous layers appear which represent the nanoclay in the rubber matrix.

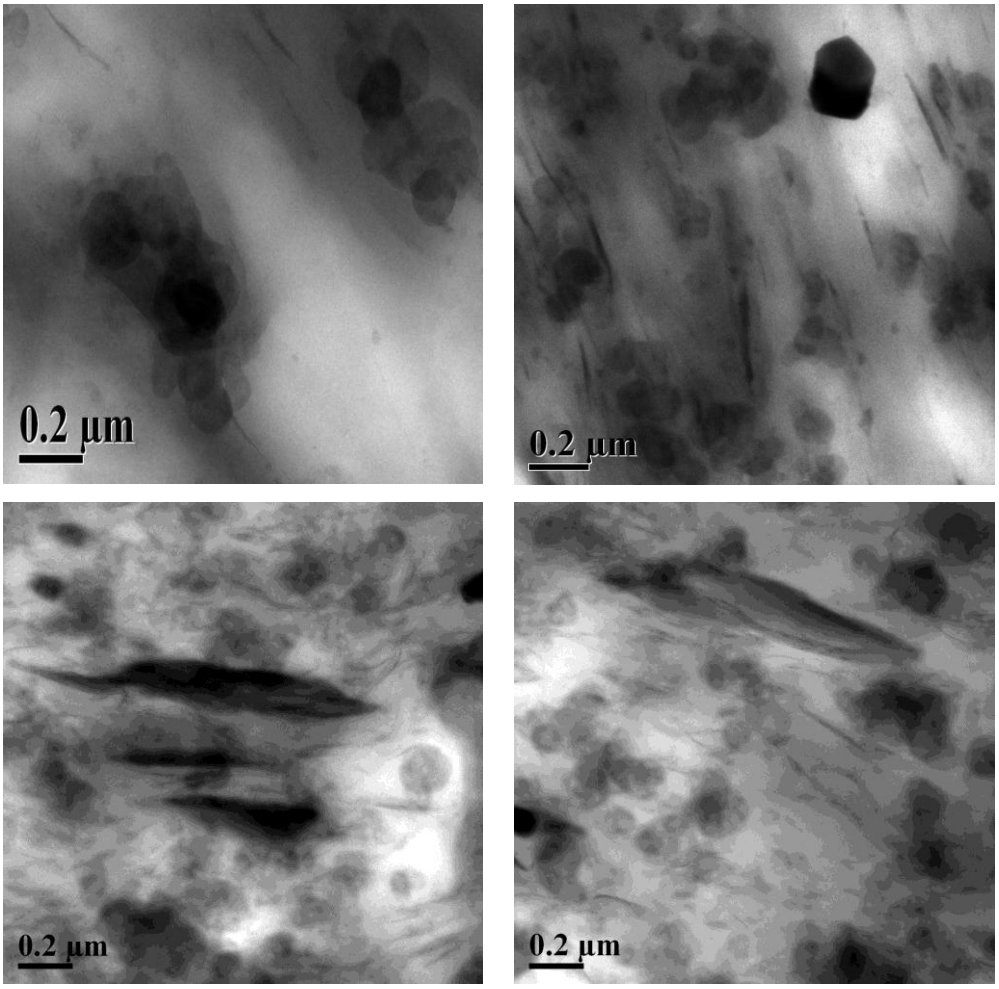

Fig. 5.25 TFM pictures of Sample M4

Sample M4 contains only 10% carbon black and 6% nanoclay hence we find that in Fig. 5.25 the filler density is considerably less but in spite of lower carbon black loading the particles are aggregated in the rubber matrix. The amount of nanoclay is more distinctly visible in the rubber matrix in Fig 5.25 in comparison to Fig.5.24, but the intercalation of the clay is not identifiable.

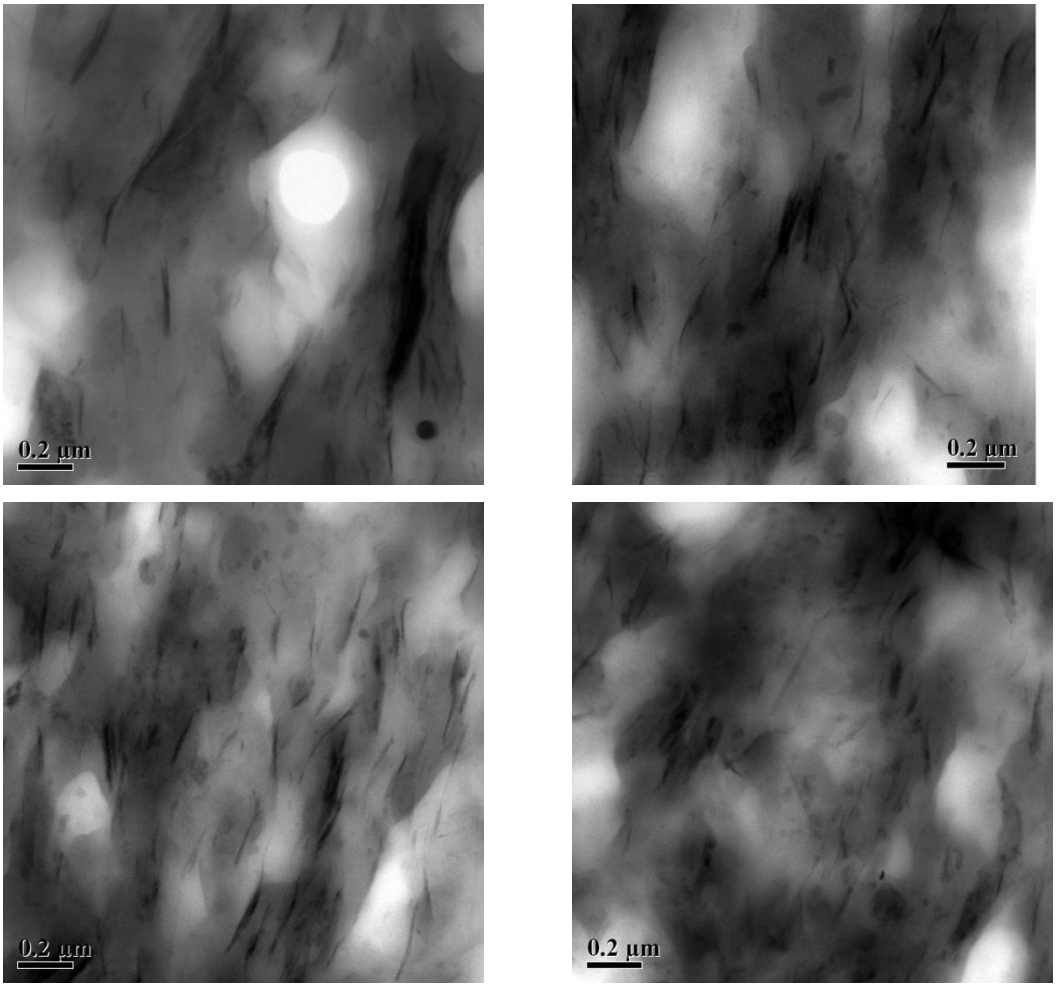

Fig. 5.26 TFM pictures of Sample M5

Fig. 5.26 is the TEM image of sample M5 that contains only nanoclay and the intercalation of nanoclay layers resulting in hair like structures is clearly visible. This aspect was also deducted by the change in basal plane spacing detected by WAXD patterns discussed earlier.

5.4.6 Atomic force microscopy

AFM was performed using the tapping mode (intermittent contact –AFM), the high sensitivity of this technique results in high resolution images of even very soft samples. For tapping AFM, feedback is usually based on amplitude modulation and the tip sample interaction passes from the 'zero-force' regime, through the attractive regime and into the repulsive regime (Eaton and West 2010). The movement of AFM tip - sample interaction through all three regimes has important implications such as the possibility of tip damage in the repulsive interaction, lateral forces are eliminated,

tip comes in contact with the fillers and tip=sample contact allows some sensing of sample properties.

In the tapping mode (IC-AFM) the most important signals are the height signals as from them one can make useful topographical deductions. They are meaningful because they give us idea about the surface roughness of the samples. AFM-studies of the samples were done to get an estimate of the roughness of the inner liner layers, while roughness would help adhesion of inner liner with adjacent layers but at the same time contribute to hysteresis losses.

Figures 5.27 to 5. 31 shows the AFM images for the various nanocomposite samples and Table 5.3 lists the surface roughness parameters of the nanocomposites, even in absence of fillers the gum rubber compound of BIIR-NR has considerable roughness addition of fillers in a way smoothens the sheet surface as revealed by the data in Table 5.3

Table 5.3 : Surface Roughness of Nanocomposites

Parameter	**Sample**					
	M0	**M1**	**M2**	**M3**	**M4**	**M5**
S_g (RM S ht) µm	0.104	0.0827	0.07	0.083	0.0619	5.93 nm
S_P(Max. Peak ht) µm	0.293	0.359	0.238	0.277	0.291	16.5 nm
S_V(Max. pit ht) µm	0.330	0.254	0.347	0.165	0.168	19.4 nm
S_Z (Max ht) µm	0.623	0.613	0.585	0.441	0.459	35.8 nm
S_a (Arithmetic Mean) µm	0.080	0.0643	0.0526	0.0672	0.0505	4.86 nm

Among the filled rubber samples it is seen that as the amount of filler in the sample reduces, the roughness parameters subside but obviously this trend cannot be extrapolated. As the presence of the nanoclay in the rubber matrix increases some of the roughness parameters go through a sharp decline. When only nanoclay is present as filler in the sample the roughness is considerably reduced, it appears that the nano filler induces a very fine scale of mixing of the polymer and consequently influences the physical properties of the sample significantly.

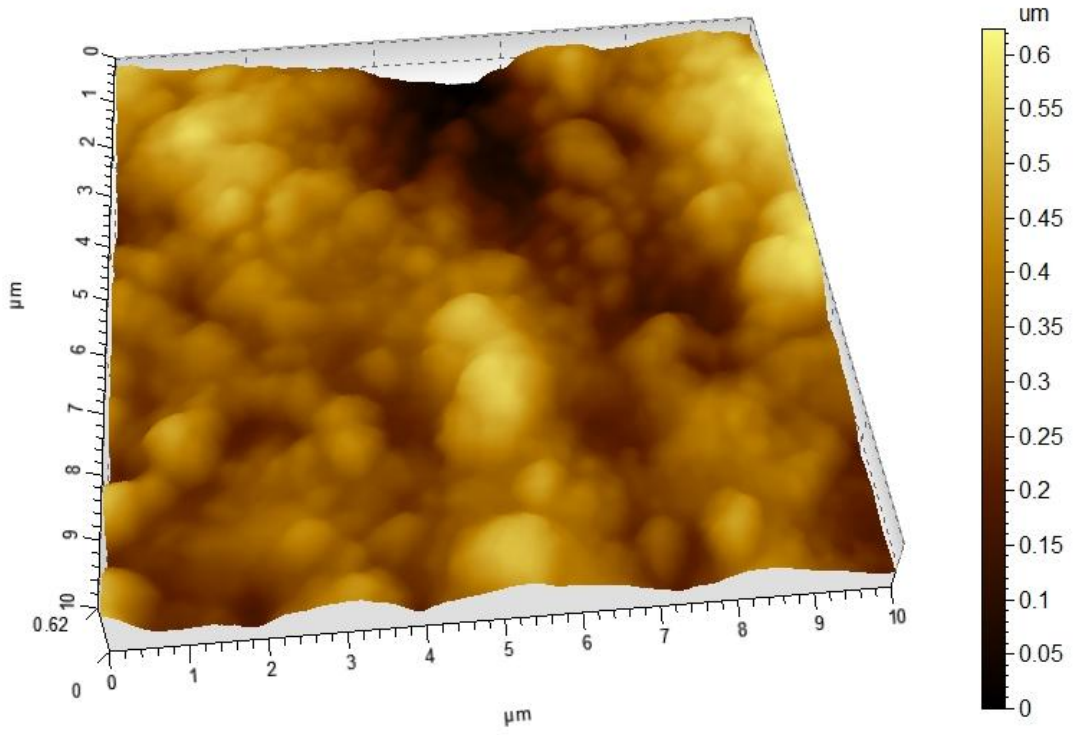

Fig. 5.27 AFM pictures of Sample M0

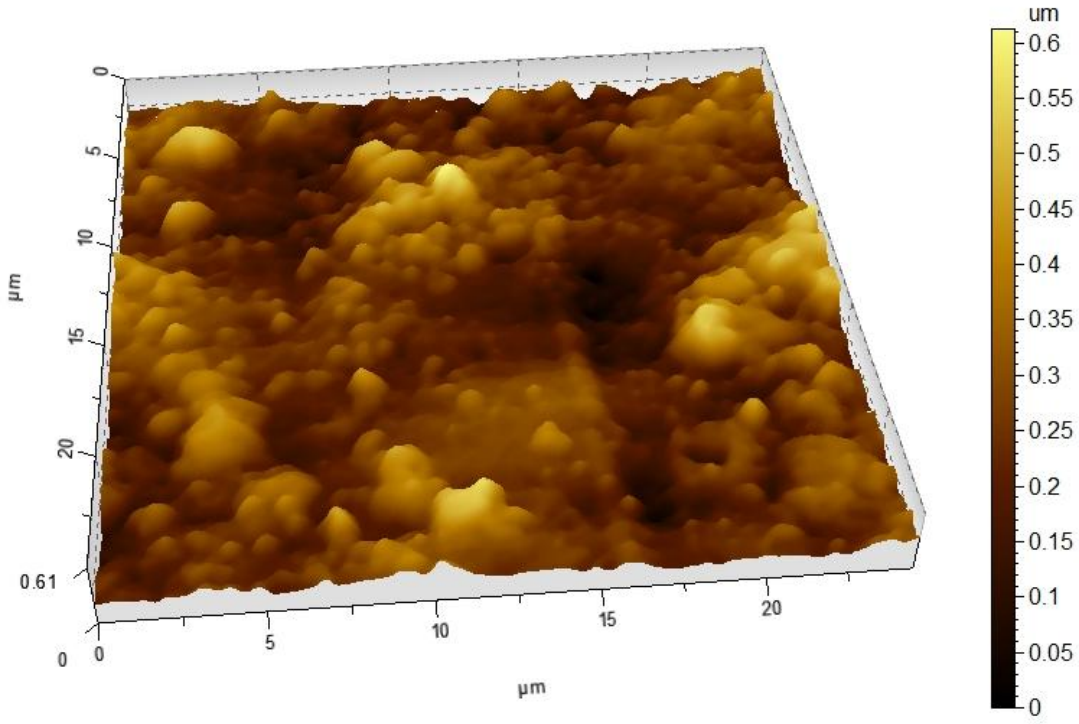

Fig. 5.28 AFM pictures of Sample M1

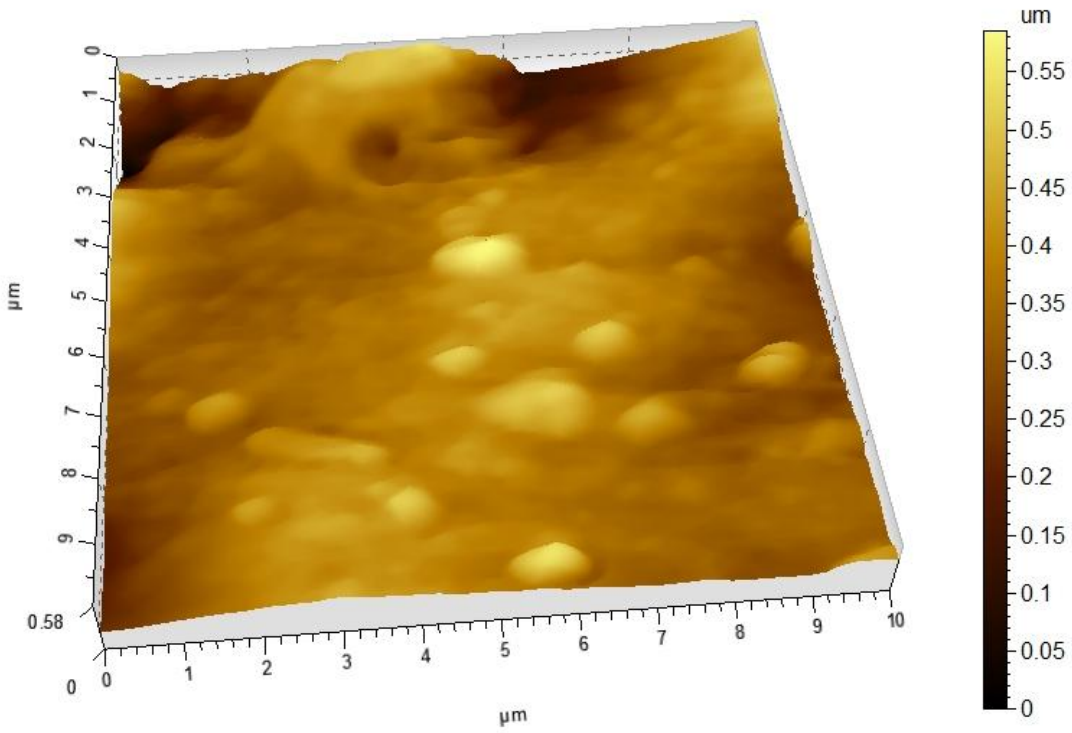

Fig. 5.29 AFM pictures of Sample M2

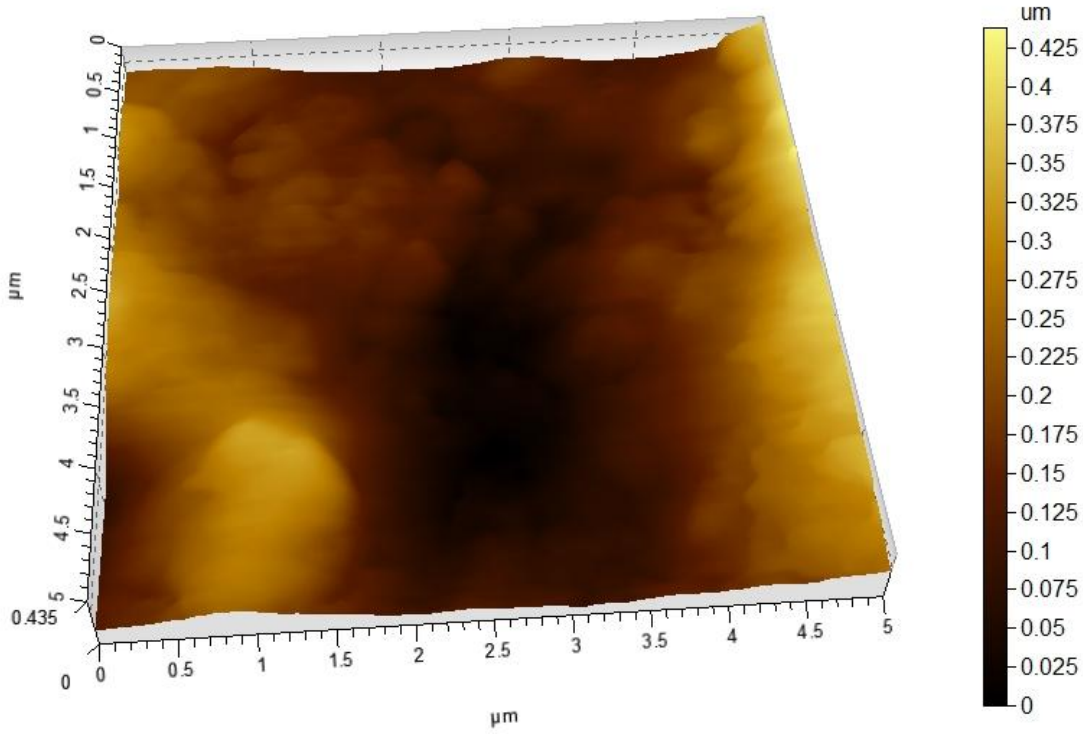

Fig. 5.30 AFM pictures of Sample M3

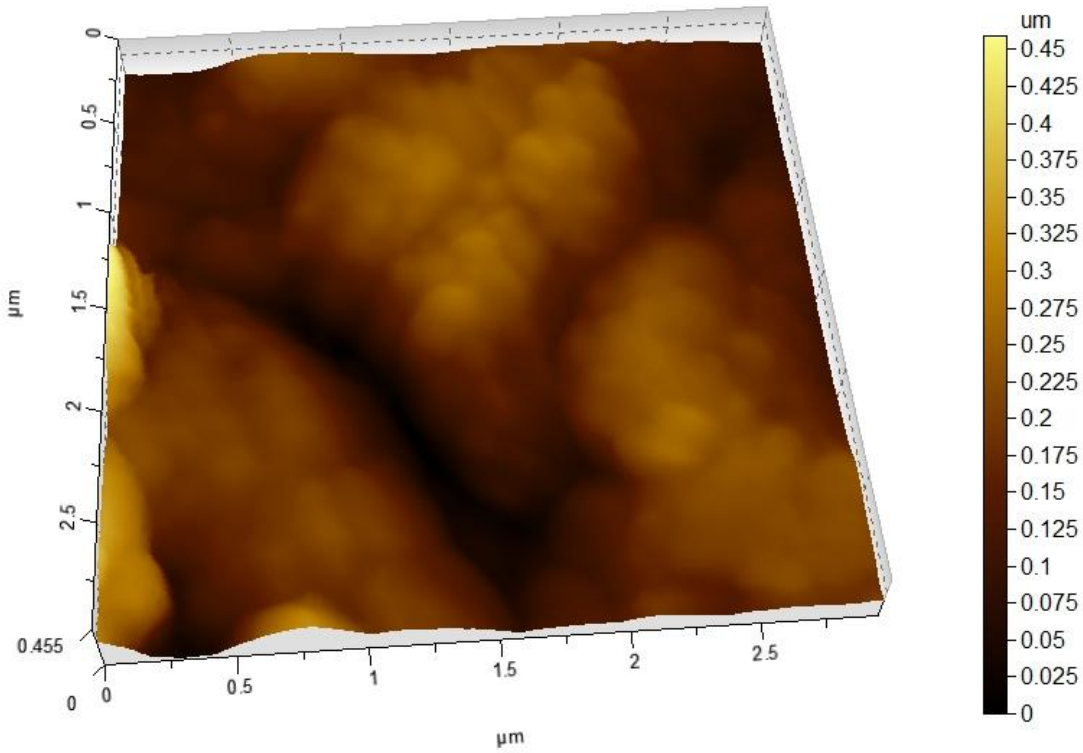

Fig. 5.31 AFM pictures of Sample M4

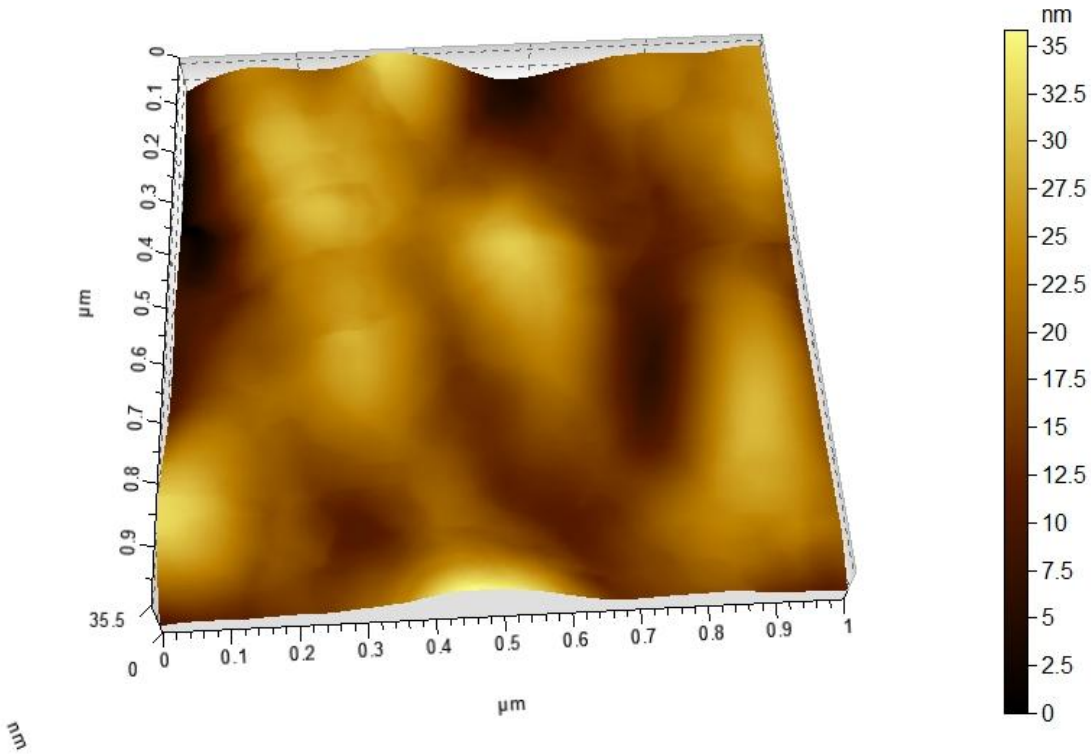

Fig. 5.32 AFM pictures of Sample M5

5.5 Conclusions

The inner liner is a very important component of modern tires and it has to fulfill certain very demanding functions. Natural rubber and bromobutyl rubber blends are industry standard material for the inner liners. Usually carbon black is the filler used but to get the appropriate reinforcement almost 40 phr filler is added that makes the liner heavy and stiff. In this investigation nanoclay was chosed as the alternative material for filler and different amount of the nanoclay along with carbon black was explored.

It was found that when carbon black was totally replaced by nanoclay only 8 phr of clay could be added and it led to good exfoliation of the clay as supported by XRD and TEM. The AFM results indicated that the roughness of samples in absence of carbon black was much less. All mechanical properties desired from the liners were also met. There is a good reason to substitute clay based inner liner in place of conventional inner liner after an economic assessment.

5.6 References

1. Bokabza L. New development in rubber reinforcement, *Kaust Gummi Kunstoff*, 2009; 23-27.
2. Chakravarty SN, Chakravarty A. Reinforcement of Rubber Compuounds with Nano-filler, *Kaust Gummi Kunstoff*, 2007; 619-622.
3. Eaton PJ, West P. Atomic force microscopy, Oxford University Press, Oxford, U.K., 2010.
4. Exxon Mobil Chemical, Exxon™ halobutyl rubber tire inner liner processing guidelines, Manual, 2014.
5. Ghosh S, Sengupta R. A., Heinrich G. Investigations on Rolling Resistance of Nanocomposite based Passenger Car Radial Tire Tread Compounds using Simulation Technique, *Tire Science and Technology*, 2011; 210-222.
6. Ghosh S, Sengupta RA, Heinrich G. High Performance Nanocomposite based on Organoclay and Blends of Different Types of SBR with BR, *Kaut Gummi Kunstst* 2011; 48- 54.
7. Ghosh S., Sengupta RA, Kaliske M. Prediction of rolling resistance for truck bus radial tires with nanocomposite based tread compounds using finite element simulation, *Rubber Chemistry and Technology*, 2014; 276-290.
8. Hua Z, Sishan W, Jain S. Polymer/Silica Nano composites: Preparation, Characterization, Properties and Applications, Chemical Reviews, 2008; 3893-3957.
9. Kang D, Kim D. Properties and Dispersion of EPDM / Modified-Organaoclay Nano composites, *Macromolecular Material & Engineering*, 2007; 329-338.
10. McBrity V, Douglas DC. Carbon Black filled natural rubber, *Macromolecules* 1991; 436-443.
11. Pal K, Pal S, Das K, Jin KK. Influence of fillers on NR/SBR/XNBR Blends, Morphology and wear, *Tribology International*, 2010; 1542-1550.
12. Pal K, Rajasekar R, Kang JD, Kim JK, Das CK. Influence of Fillers on NR/SBR/SNBR Blends. Morphology and Wear, *Nanoscience and Nanotechnology*, 2010; 1-12.

13. Pal K, Rajasekar R, Kang JD, Zhang ZX, Kim JK, Das CK. Effect of Epoxidized Natural Rubber-Organoclay Nano-Composites on NR/high Styrene Rubber Blends with fillers, ICFAI Journal of Science & Technology, 2008; 17-29.
14. Pal K, Rajasekar R, Kang JD, Zhang ZX, Pal SK, Kim JK, Das CK. Effect of Fillers on Natural Rubber/high Styrene Rubber Blends with Nano Silica : Morphology and Wear, *Materials and Design*, 2010; 25-34.
15. Paul DR, Robeson LM. Polymer nanotechnology: Nanocomposites, *Journal of Polymer*, 2008; 3187-3204.
16. Pavlidou S, Papaspyrides CD. A review on polymer layered silicate nanocomposites, *Progress in polymer science*, 2008; 1119-1198.
17. Ruiz-Hitzkya E, Van Meerbeek A. Clay Mineral and Organoclay-Polymer Nano-Composites, In: Bergaya F, Theng BKG, Lagaly G (Editors). *Handbook of Clay Science*, Elsevier, Amsterdam, 2006; 583-621.
18. Sadhu S, Bhowmick AK. Morphology study of rubber based nanocomposites by transmission electron microscopy and atomic force microscopy, *Journal of Material Science*, 2005; 1633-1642.
19. Sadhu S, Bhowmick AK. Preparation and characterization of styrene butadiene rubber based nanocomposite: Influence of structural and processing parameters, *Journal of Applied Polymer Science*, 2004; 698.
20. Sinha RS, Okamdo M. Polymer layered silicate nanocomposites: A review from preparation to processing, *Progress in polymer science*, 2003; 1639-1641.
21. Song Y, Zheng Q. Linear viscoelasticity of polymer melts filled with nano-sized fillers, *Journal of Polymer*, 2010; 3262-3268.
22. Susteric Z, Tomaz K. Elastomer-Clay Nano Composites: Effect of Elastomer polarity, *Macromolecular Symposia*, 2010; 296, 311-315.
23. Thomas S, Stephen R. Rubber Nanocomposites Preparation, Properties and Applications, John Wiley and Sons, Singapore, 2010; ISBN: 978-0-470-82345-3.
24. Usiki A, Kawasumi M, Kojima Y, Okada A, Fukushima Y, Kurachi T, Kamigaito O. Synthesis of Nylon 6-clay hybrid, *Journal of Material Science*, 1993; 1179-1184.